CO-induced decomposition of small Pt particles in K-LTL zeolite

B.L. Mojet and D.C. Koningsberger

Debye Institute, Department of Inorganic Chemistry and Catalysis, Utrecht University, PO Box 80083, 3508 TB Utrecht, The Netherlands

Received 29 March 1996; accepted 12 April 1996

Reduced Pt/K-LTL has been studied with XAFS spectroscopy before and after CO admission at room temperature. The results of the EXAFS data-analysis show that after reduction very small platinum metal particles are present consisting of five to six atoms. CO admission at room temperature leads to complete decomposition of the platinum metal particles and the formation of a platinum carbonyl cluster most probably stabilised by the zeolite walls. Modelling shows that the platinum carbonyl cluster just fits inside the pores of the zeolite LTL. Analysis of the white line intensities of platinum L_{II} and L_{III} X-ray absorption edges reveals that after reduction and in the presence of chemisorbed hydrogen the platinum metal particles in Pt/K-LTL have 0.12% more d-band vacancies than bulk platinum metal. This value increases to 0.34% after CO admission implying π-backdonation from platinum to CO, a positive charge on Pt in the newly formed cluster or a combination of both. The results of this study have a large impact on the interpretation of existing literature FTIR CO data obtained on Pt/K-LTL. The results question the validity of CO chemisorption carried out to determine the dispersion of very small platinum particles.

Keywords: Pt–CO complexes; EXAFS spectroscopy; Pt/K-LTL; CO chemisorption on Pt

1. Introduction

In the last years much attention has been paid to the characterisation of catalytic and electronic properties of Pt/K-LTL, as this catalyst demonstrates a unique activity and selectivity for aromatisation of *n*-hexane to benzene [1]. XAFS studies revealed the presence of five-to-six-atom metal clusters in interaction with support oxygen atoms [2], and FTIR-studies of adsorbed CO were used to determine electronic properties of the catalyst [3–6]. Despite numerous experiments, interpretation of the infrared data is still a matter of debate. The observed CO-band structure was attributed to particle size effects [7], ion–dipole interactions between CO and K^+ [8] and electronic effects directly from the zeolite on the metal particles [3–5]. Recently, Stakheev and co-workers presented an infrared study of CO adsorbed on reduced Pt/K-LTL as function of CO partial pressure [9]. In order to explain their results and results obtained by other groups, they suggested the formation of new, neutral platinum carbonyl clusters inside the zeolite. Although it is known that anionic platinum carbonyl clusters can be formed from precursor complexes and CO [10–13], literature provides no information on the formation of platinum carbonyl clusters from reduced platinum particles and carbon monoxide.

To investigate the suggested formation of platinum carbonyl clusters from reduced platinum particles in zeolite LTL, we performed EXAFS experiments on the reduced catalyst before and after CO adsorption at 1 atm. The results of this study are of great importance for the application of CO-adsorption to characterise very small platinum particles in zeolite LTL.

2. Experimental

2.1. Catalyst preparation

The K-LTL zeolite was obtained from Linde and repeatedly washed with water until the pH of the solution was 9.5. The resulting K-LTL zeolite was calcined at 225°C and contained 8.5 wt% Al and 11.8 wt% K. Platinum was added by incipient wetness impregnation of $[Pt(NH_3)_4](NO_3)_2$ followed by drying at 120°C. After reduction in flowing hydrogen at 300°C, the resulting catalyst contained 1 wt% Pt and had a H/Pt of 0.89 as determined with H_2 chemisorption at room temperature.

2.2. XAFS experiments

The catalyst was characterised by XAFS spectroscopy at the SRS Daresbury, UK at Wiggler Station 9.2, using a Si(220) double crystal monochromator. The measurements were done in transmission mode using ion chambers filled with Ar to have a μx of 20% in the first and a μx of 80% in the second ion chamber.

The sample was pressed into a self-supporting wafer (calculated to have an absorbance of 2.5) and placed in an in situ cell [14]. It was dried at 120°C and subsequently reduced at 300°C (heating rate 5°C/min) for 1 h in flowing hydrogen (purified and dried). Subsequently, the sample was cooled down under flowing H_2 and spectra were taken at liquid nitrogen temperature. After the sample was allowed to warm up to room temperature it was exposed to a flow of CO/He (1/1, dried) for 15 min, and allowed to stand for 1 h at room temperature. XAFS

spectra were taken at liquid nitrogen temperature in the presence of CO/He.

2.3. XAFS data analysis

The pre-edge background was approximated by a modified Victoreen curve [15], the background was subtracted using cubic spline routines [16]. Spectra were normalised by dividing the absorption intensity by the height of the absorption edge at 50 eV above the edge. The final EXAFS function was obtained by averaging the individual background-subtracted and normalised data (four scans).

Data for the phase shifts and backscattering amplitudes were obtained from reference compounds. Pt-foil was used as a reference for Pt–Pt contributions, $Na_2Pt(OH)_6$ was used for Pt–O contributions [17]. To analyse adsorbed CO, Pt–C and multiple scattering Pt–O* references are necessary [18]. XAFS data of crystalline $Ir(CO)_{12}$ were used to extract Ir–C and multiple scattering Ir–O* backscattering amplitudes and phase shifts. As phase shift and backscattering amplitude are transferable between Pt and Ir these data could be used to calculate a model spectrum for Pt–C and Pt–O* contributions [19].

The fit parameters were determined by multiple shell fitting in r-space [20]. Different backscatterers were identified by applying the difference file technique using phase-corrected Fourier transforms [21].

3. Results

The XAFS data of the reduced catalyst before and after CO exposure are shown in fig. 1a. It can be seen that the data have a good signal to noise ratio. Further, at low k-values there clearly are differences in amplitude and nodes of the EXAFS for both samples. Comparison of the Fourier transforms in k^3-weighting (fig. 1b) reveals that both amplitude and imaginary part of the two spectra differ significantly. Between 2.0 and 4.0 Å the amplitude is lower after CO adsorption, while in the region 0.5–2.0 Å it has increased. Also, the nodes in the imaginary part of the Fourier transform are shifted upon CO exposure, thus indicating that the structure of the catalyst has altered.

Analysis of the data in r-space of the reduced Pt/K-LTL (table 1) shows that besides a Pt–Pt contribution at 2.74 Å also a long Pt–O contribution at a distance of 2.68 Å is present. This can be explained by the presence of very small platinum clusters inside the zeolite pores; a large fraction of the platinum atoms are in contact with the support. The origin of the long metal–support oxygen contribution has been discussed before and is proven to be caused by the presence of interfacial hydrogen [2]. The analysis parameters are in very good agreement with earlier published analysis of similar Pt/K-LTL [2].

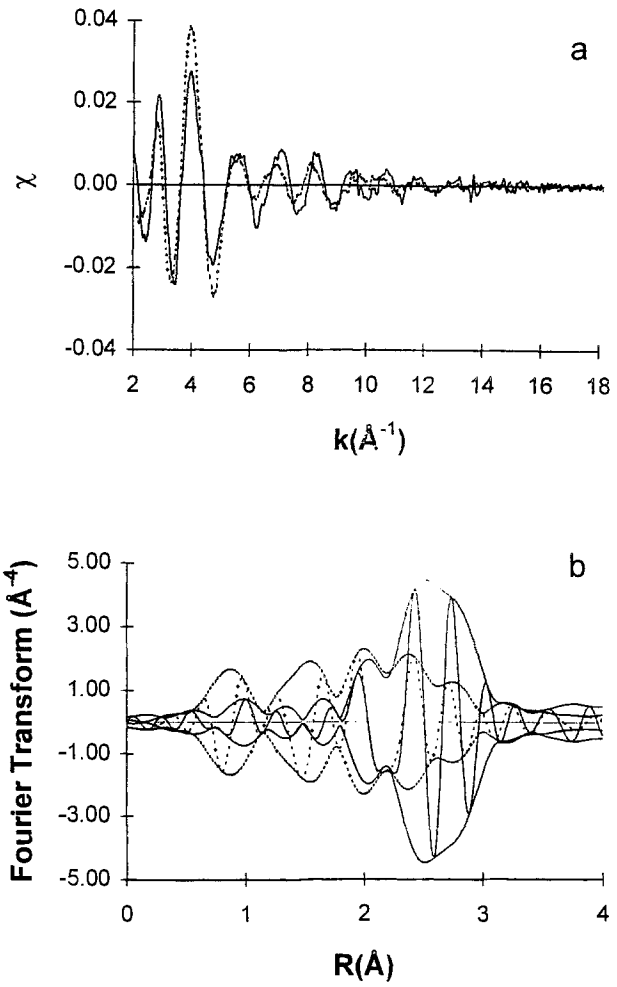

Fig. 1. (a) Raw EXAFS data of Pt/K-LTL reduced at 300°C (solid line) and after CO admission (dotted line). (b) Fourier transform (k^3, Δk: 3.2–12.7 Å^{-1}) of data shown in (a).

Fig. 2a shows the Fourier transforms of the experimental data and calculated spectrum of Pt/K-LTL after CO exposure. Fitting of the spectra in r-space (k^1-weighting, r-range: 0.5–4.0 Å) reveals Pt–Pt, Pt–C, Pt–O*, and Pt–O contributions as given in table 2. The resemblance of the data and calculated spectrum in k-space (fig. 2b) indicates that no additional backscatterers are present. All contributions were tested for their relevance to the model spectrum, the statistical significances being over 85%. To determine the quality of fit

Table 1
Structural parameters for Pt/K-LTL reduced at 300°C as determined from EXAFS data analysis: r-space fit, k^2 weighting, Δk: 3.2–14.0 Å^{-1}, Δr: 1.0–3.5 Å) [a]

Backscatterer	Coordination number	Distance (Å)	$\Delta\sigma^2$ (Å^2 × 10^{-3})	ΔE_0 (eV)
Pt	4.2 ± 0.5	2.74 ± 0.02	3.5 ± 0.1	−1.6 ± 0.5
O	1.7 ± 0.2	2.68 ± 0.02	0.9 ± 0.1	5.0 ± 0.8

[a] Variance absolute part FT: 1.3%, variance imaginary part FT: 0.7%. Errors are estimated

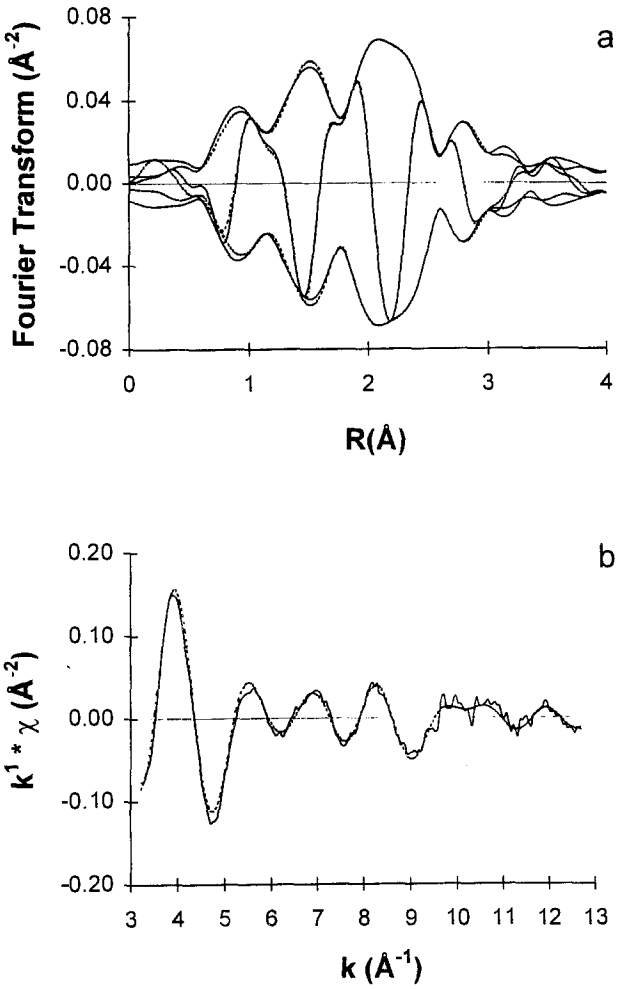

Fig. 2. (a) Fourier transform (k^1, Δk: 3.2–12.7 Å^{-1}) of EXAFS data of Pt/K-LTL reduced at 300°C and exposed to CO (solid line) and calculated spectrum with parameters given in table 2 (dotted line); (b) EXAFS data (k^1-weighted) of Pt/K-LTL reduced at 300°C and exposed to CO (solid line) and calculated spectrum (dotted line).

for all separate contributions the difference file technique was applied [21]. As the total XAFS spectrum is a sum of the spectra of each individual component, the individual contributions can be compared with the residual spectrum after subtracting all other components from the experimental data (fig. 3). It can be seen that both imaginary and absolute parts of the Fourier transforms of the invidual components and the difference spectra are in good agreement for all backscatterers.

The normalised Pt L_{III} and L_{II} white lines for Pt-foil, Pt/K-LTL after reduction and after subsequent CO admission are given in fig. 4. The intensities for both L_{III} and L_{II} increased upon CO exposure. The increased white line intensity of the reduced sample compared to the platinum foil is due to chemisorbed hydrogen on the sample [22–24]. To quantify the differences in white line intensity between the catalysts and a platinum foil, the approach described by Mansour et al. was used [25]. After subtracting the platinum foil data from the catalyst data, the resulting curves were numerically integrated between −2 and +17 eV for both the L_{III} ($\Delta A'_3$) and the L_{II} ($\Delta A'_2$) edge. The areas were combined to give the fractional change in the number of d-band vacancies relative to platinum bulk metal: $f_d = (2.51\Delta A'_3 + 1.29\Delta A'_2)/19.2$. The resulting f_d value for reduced Pt/K-LTL was 0.12, and after CO exposure 0.34.

Table 2
Structural parameters for Pt/K-LTL reduced at 300°C after CO admission as determined fromwith EXAFS data-analysis: r-space fit, k^1 weighting, Δk: 3.2–12.7 Å^{-1}, Δr: 0.5–4.0 Å [a]

Backscatterer	Coordination number [b]	Distance [c] (Å)	$\Delta\sigma^2$ [b] (Å^2 × 10^{-3})	ΔE_0 [b] (eV)
Pt	2.2 ± 0.4	2.67 ± 0.02	4.8 ± 0.5	12.0 ± 2
O*	2.3 ± 0.4	2.86 ± 0.08	19.9 ± 2.0	1.6 ± 0.5
C	2.4 ± 0.4	1.92 ± 0.02	2.2 ± 0.3	−1.8 ± 0.5
O	1.3 ± 0.3	2.28 ± 0.02	5.5 ± 0.6	−5.8 ± 0.8

[a] Variance absolute part FT: 0.8%, variance imaginary part FT: 0.3%.
[b] Estimated errors.
[c] Calculated mathematical errors.

4. Discussion

Fig. 1 shows that the geometrical structure of reduced platinum in zeolite LTL upon exposure to CO is changed completely. There are striking differences when comparing the coordination parameters as given in tables 1 and 2. Firstly, for Pt/K-LTL after CO admission the Pt–Pt distance has contracted from 2.74 to 2.67 Å, together with a decrease of Pt–Pt coordination number from 4.2 to 2.2. Both features indicate the decomposition of the metallic platinum particles into smaller entities.

The inner potential correction (ΔE_0) of the Pt–Pt contribution is quite large compared to reduced Pt/K-LTL. This might indicate a change in charge on platinum, which results in a different inner-potential correction for the Pt–Pt contribution. Analysis of the white line intensities of the Pt L_{III} and L_{II} X-ray absorption resulted in an increase of the fractional change in the number of d-band vacancies from 0.12 to 0.34% when the catalyst was exposed to CO. Thus, the platinum atoms have a lower electron density after CO adsorption. This can be explained by either π-backdonation from platinum to CO, a positive charge on Pt or a combination of both. Regardless of the origin, the large inner potential correction and the increased white line intensity both point to a decreased electron density on platinum.

Furthermore, the new Pt–C and Pt–O* contributions indicate that CO molecules coordinated to Pt are present. The difference of 1 Å between C and O* is in good agreement with the intramolecular distance in CO [18]. The corresponding coordination numbers of the Pt–C and Pt–O*, 2.4 and 2.3 respectively, are within the limits of accuracy in accordance with two linearly bound CO molecules. For the Pt–O* contribution the error in dis-

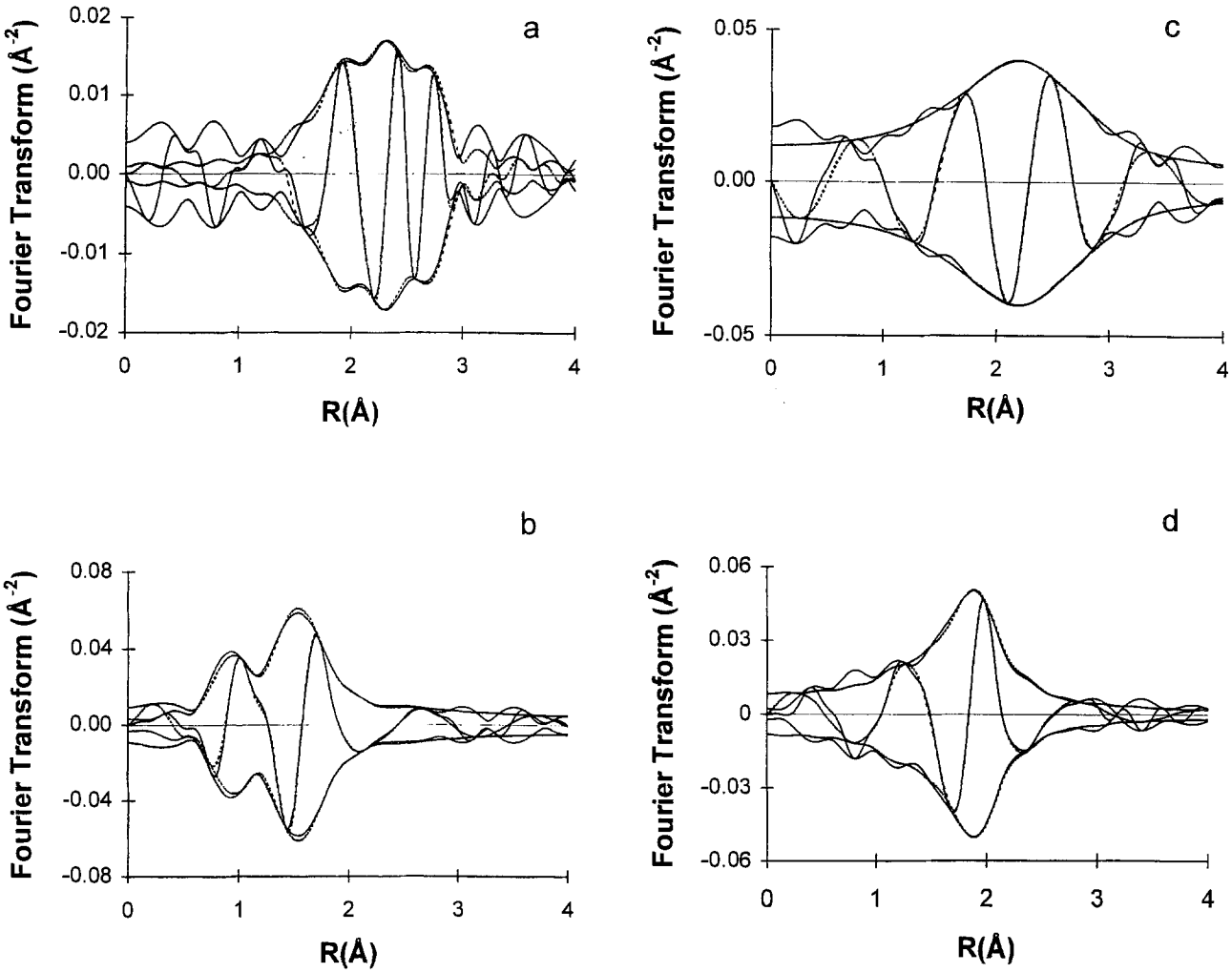

Fig. 3. Fourier transform (k^1-weighted, Δk: 3.1–14.0 Å^{-1}) of each individual calculated EXAFS contribution and difference file of the EXAFS spectrum of reduced Pt/K-LTL after admission of CO. (a) Pt–Pt: calculated contribution (dotted line) and EXAFS data minus calculated ((Pt–C) + (Pt–O*) + (Pt–O)) (solid line); (b) Pt–C: calculated contribution (dotted line) and EXAFS data minus calculated ((Pt–Pt) + (Pt–O*) + (Pt–O)) (solid line); (c) Pt–O*: calculated contribution (dotted line) and EXAFS data minus calculated ((Pt–Pt) + (Pt–C) + (Pt–O*)) (solid line); (d) Pt–O: calculated contribution (dotted line) and EXAFS data minus calculated ((Pt–Pt) + (Pt–C) + (Pt–O*)) (solid line).

tance is larger than for the other contributions. The large Debye–Waller factor of 19.9×10^{-3} also indicates a higher disorder in the Pt–O* backscattering function. These two features can be explained by the fact that (linear) bound CO on a very small platinum entity can bend freely, thus creating a larger deviation in the average Pt–O* distance which is reflected in both the uncertainty in distance and the high Debye–Waller factor.

A fourth contribution in the Fourier transform of the data is present at 2.28 Å, most likely due to support oxygen atoms. It was also tried to fit the spectrum with a Pt–C contribution, thus accounting for a possible third coordinated CO molecule, but the goodness of fit was lower than with a Pt–O contribution. Furthermore, if there was a Pt–C contribution at 2.28 Å, there also should be a significant Pt–O* contribution at around 3.0–3.4 Å. However, no O* contribution could be detected in the region 3.0–3.4 Å. Besides this, the small shift in inner potential (−5.8 eV) indicates that the calculated Pt–O contribution may be the correct one. This suggests a stabilising effect of the zeolite oxygen atoms on the Pt–carbonyl entity.

The calculated spectrum with four contributions agrees in k-space as well as r-space with the experimental data, which implies that higher coordination shells are absent. Although the Pt–Pt coordination number and distance show good resemblance with the coordination in a Chini-complex ($[Pt(\mu CO)(CO)_2]_n^{2-}$) [26], the number of CO ligands is not similar, since in a Chini-complex each platinum atom is surrounded by three carbon atoms (two bridged bound, one linear coordinated). This indicates that a Pt–carbonyl cluster has formed familiar to a Chini-complex, with CO coordinated to platinum in linear position only.

The coordination parameters found in this study point to a structure of $[Pt(\text{linear-CO})_2]_3$ stabilised by the

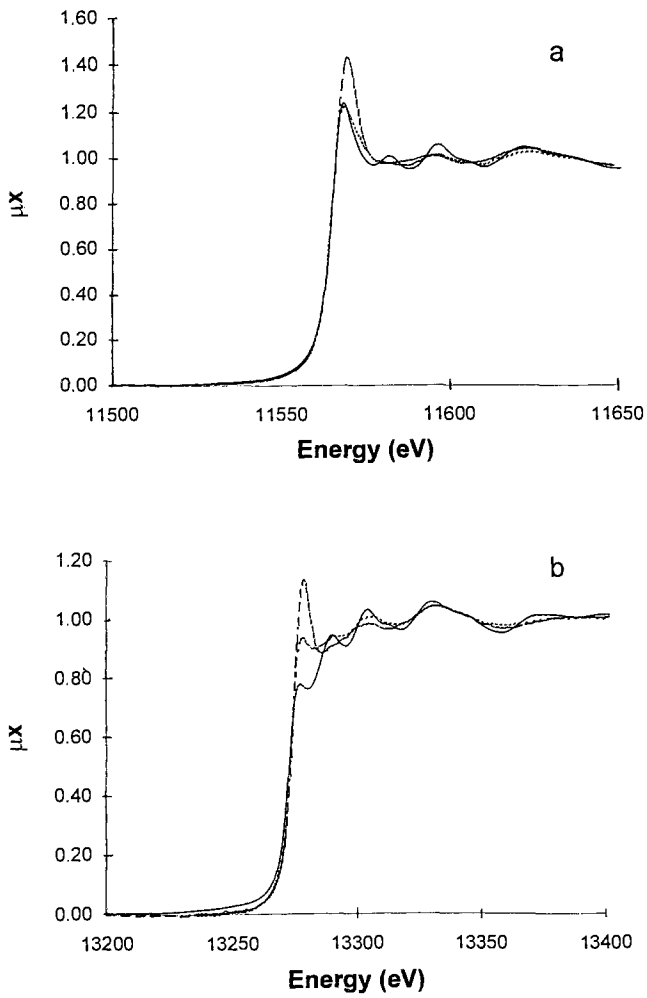

Fig. 4. Normalised white lines of X-ray L_{III} (a) and L_{II} (b) absorption edges of Pt-foil (solid line), reduced Pt/K-LTL before (dotted line) and after exposure to CO (dashed line).

zeolite walls. A possible geometrical structure of the Pt–carbonyl cluster inside zeolite LTL is schematically shown in fig. 5. The Pt–Pt distance of 2.67 Å and Pt–O distance of 2.28 Å taken into account results in a cluster that exactly fits in the small LTL-pore opening of 7.1 Å.

For very small supported rhodium particles it is known that the metal particles decompose into mononuclear carbonyl clusters [27]. For palladium in zeolite Y it was reported that the metal particles grew under CO atmosphere, giving large $Pd_x(CO)_y$ clusters that just fit inside the supercages of zeolite Y [28]. Recently, it was suggested based on FTIR experiments that the geometrical structure of platinum in zeolite LTL should change upon CO exposure [9]. The authors suggested the formation of a new neutral Pt–carbonyl instead of a Chini-complex, as the FTIR spectra of their sample significantly differed from the IR-data known for negatively charged Chini-complexes [29].

This study clearly shows that the geometrical structure of small platinum particles inside zeolite LTL changes upon admission of CO at 1 atm. The platinum particles decompose upon exposure to CO into smaller Pt–carbonyl entities which seem to be stabilised by the zeolite walls. The L_{III} and L_{II} white lines of the sample show a decreased electron density on platinum after CO admission. However, it is not clear whether this is due to π-backdonation or a cationic charge on the platinum atoms.

Preliminary results of additional XAFS experiments indicate that the decomposition of platinum in zeolite LTL is probably particle size dependent. Larger particles do not show a decreased Pt–Pt coordination or a contracted Pt–Pt distance after CO admission. Further, previous infrared studies showed a significant effect of water on the actual CO-FTIR spectrum [8]. For this reason, the influence of other experimental parameters (like water and hydrogen) on the decomposition of small platinum particles in zeolite LTL is currently investigated with XAFS spectroscopy.

This study has revealed that CO chemisorption for the characterisation of platinum particles in zeolite LTL has to be applied very carefully. Although previous published experimental results of FTIR studies on Pt/LTL are still valuable, the interpretation of the data has become more complicated. Our group is combining XAFS and CO FTIR experiments on the same catalysts

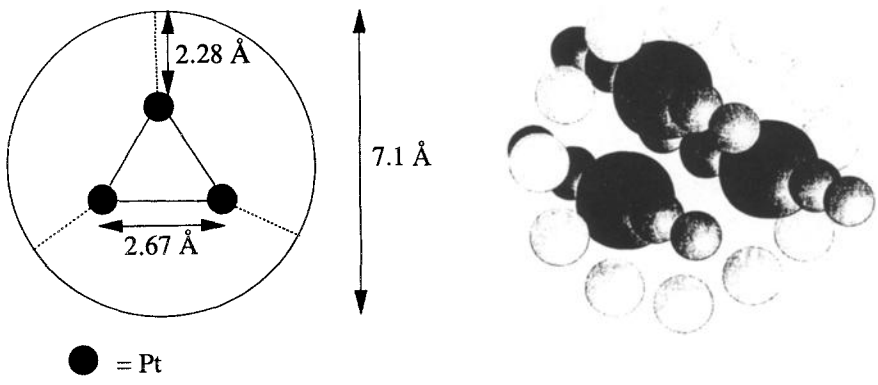

Fig. 5. Proposed geometrical structure of a Pt–carbonyl cluster inside zeolite LTL.

under the same experimental conditions. The influence of temperature and presence of H_0 on the formation of the platinum carbonyl complex is being studied. The results will be published in due course.

5. Conclusion

XAFS experiments on reduced Pt/K-LTL before and after CO admission reveal that the small platinum particles decompose upon CO exposure. This leads to small $[Pt(CO)_2]_3$ entities that are stabilised by the zeolite pore walls. These results give a new insight in the application of CO adsorption to characterise very small metal particles in zeolites.

Acknowledgement

The authors would like to thank Jeff Miller (Amoco Oil) for preparing the catalyst, Bob Leliveld, Ad van der Eerden, Jeroen van Bokhoven (Utrecht University) and Gert van Dorssen (Daresbury Laboratory) for their company and assistance at Daresbury Laboratory.

References

[1] J.R. Bernard, in: *Proc. 5th Int. Congr. on Zeolites*, ed. L.V.C. Rees (Heyden, London, 1980) p. 686.
[2] M. Vaarkamp, F.S. Modica, J.T. Miller and D.C. Koningsberger, J. Catal. 144 (1993) 611.
[3] B.L. Mojet, M.J. Kappers, J.T. Miller and D.C. Koningsberger, *Proc. 11th ICC*, accepted.
[4] A. de Mallmann and D. Barthomeuf, Stud. Surf. Sci. Catal. 46 (1989) 429.
[5] W.J. Han, A.B. Kooh and R.F. Hicks, Catal. Lett. 18 (1993) 193.
[6] L.M. Kustov, D. Ostgard and W.M.H. Sachtler, Catal. Lett. 9 (1991) 121.
[7] M.J. Kappers, J.T. Miller, D.C. Koningsberger, J. Phys. Chem., in press.
[8] M.J. Kappers, M. Vaarkamp, J.T. Miller, F.S. Modica, J.H. van der Maas and D.C. Koningsberger, Catal. Lett. 21 (1993) 235.
[9] A.Yu. Stakheev, E.S. Shpiro, N.I. Jaeger and G. Schulz-Ekloff, Catal. Lett. 34 (1995) 293.
[10] A. de Mallmann and D. Barthomeuf, Catal. Lett. 5 (1990) 293.
[11] H. Bischoff, N.I. Jaeger, G. Schulz-Ekloff and L. Kubelkova, J. Mol. Catal. 80 (1993) 95.
[12] J.-R. Chang, Z. Xu, S.K. Purnell and B.C. Gates, J. Mol. Catal. 80 (1993) 95.
[13] G.-J. Li, T. Fujimoto, A. Fukuoka and M. Ichikawa, Catal. Lett. 12 (1992) 171.
[14] M. Vaarkamp, B.L. Mojet, M.J. Kappers, J.T. Miller and D.C. Koningsberger, J. Phys. Chem. 99 (1995) 16067.
[15] M. Vaarkamp, I. Dring, R.J. Oldman, E.A. Stern and D.C. Koningsberger, Phys. Rev. B 50 (1994) 7872.
[16] J.W. Cook Jr. and D.E. Sayers, J. Appl. Phys. 52 (1981) 5024.
[17] F.W.H. Kampers, PhD Thesis, Eindhoven University of Technology, Eindhoven, The Netherlands (1989).
[18] F. van Zon, PhD Thesis, Eindhoven University of Technology, Eindhoven, The Netherlands (1988).
[19] B. Lengeler, J. Phys. (Paris) C 8 47 (1986) 75.
[20] M. Vaarkamp, B.L. Mojet and D.C. Koningsberger, to be published.
[21] J.B.A.D. van Zon, D.C. Koningsberger, H.F.J. van 't Blik and D.E. Sayers, J. Chem. Phys. 82 (1985) 5742.
[22] F.W. Lytle, R.B. Greegor, E.C. Marques, V.A. Biebesheimer, D.R. Sandstrom, J.A. Horsley, G.H. Via and J.H. Sinfelt, ACS Symp.Ser. 288 (1985) 280.
[23] M.G. Samant and M. Boudart, J. Phys. Chem. 95 (1991) 4070.
[24] B.J. McHugh, G. Larsen and G.L. Haller, J. Phys. Chem. 94 (1990) 8621.
[25] A.N. Mansour, J.W. Cook Jr. and D.E. Sayers, J. Phys. Chem. 88 (1984) 2330.
[26] G.J. Li, T. Fujimoto, A. Fukuoka and M. Ichikawa, J. Chem. Soc. Chem. Commun. (1991) 133.
[27] H.F.J. van 't Blik, J.B.A.D. van Zon, T. Huizinga, J.C. Vis, D.C. Koningsberger and R. Prins, J. Am. Chem. Soc. 107 (1985) 3139.
[28] L.L. Sheu, H. Knözinger and W.M.H. Sachtler, J. Am. Chem. Soc. 111 (1989) 8125.
[29] G. Schulz-Ekloff, R.J. Lipski, N.I. Jaeger and P. Hulstede, Catal. Lett. 30 (1995) 65.